CORROSION RESISTANCE OF POWER PLANT COMPONENTS AFTER SERVICE

Authors: ***P. GOGOLA*, T. KUNÍKOVÁ** , M. DOMÁNKOVÁ*, Ľ. ČAPLOVIČ*, M. VACH*, J. JANOVEC****

Workplace: **** Institute of Materials Science, Faculty of Materials Science and Technology, Slovak University of Technology,***

Address: ***Bottova 24, 917 24 Trnava, Slovak Republic***

***** PSL, a.s., Robotnícka ul., 017 01 Považská Bystrica, Slovak Republic***

Abstract:

Three austenitic steels (18Cr-8Ni, 18Cr-10Ni, and 21Cr-30Ni) exploited for long-terms at temperatures between 600 and 800°C were investigated. In the investigation, EPR-DL and oxalic acid etch corrosion tests, metallography, scanning electron microscopy, transmission electron microscopy, selected area electron diffraction, and energy dispersive X-ray spectroscopy were used. In the severe sensitized 18Cr-8Ni steel, small densely arranged intergranular particles mostly of $M_{23}C_6$ were found. The 18Cr-10Ni steel was classified as less sensitized compared to the 18Cr-8Ni steel due to the presence of larger discrete grain boundary particles additionally to small densely arranged particles. In the unsensitized 21Cr-30Ni steel, huge discrete clusters often exceeding 10 μm were observed at the grain boundaries. The clusters were found to consist of large Cr-rich $M_{23}C_6$ and small Ti-rich MC particles.

Key words: austenitic steels, corrosion tests, TEM, secondary phases

INTRODUCTION

More than hundred years of experiences stay behind the good mechanical properties and corrosion resistance of austenitic steels. The properties of these steels make it possible to use them in aggressive and hot environments as components of power generating nuclear plants and other energy systems. They are also used in the food, paper, chemical and petrochemical industries. In order to avoid the failure of components made of austenitic steels due to extreme service conditions, the steels high microstructural stability is required. The stability of the microstructure is ensured with alloying elements, mainly chromium and nickel. Nickel provides the formation of an austenitic microstructure at all temperatures and chromium provides the good corrosion resistance. Both elements are characteristic for the 300 series of austenitic steels. Also other alloying elements are present in the steel, so it is important to carry out a solution treatment of these steels to obtain a homogenous microstructure. The temperature of the solution treatment was reported to range between 1000 and 1150°C [1-4]. In case of the steels stabilized with Nb (347) or Ti (316Ti, 321) the stabilization treatment follows ensuring the precipitation of NbC and TiC and inhibiting from the formation of Cr-rich $M_{23}C_6$. The temperature of the stabilization treatment is around 900°C, but it varies according to the type of the steel [4,5]. The precipitation of Cr-rich particles causes the formation of Cr-depletion zones responsible for the steel sensitization and for the intergranular corrosion during service in the temperature range of 450-850°C. The fine carbides and/or carbonitrides of Nb and/or Ti increase also the strength and creep resistance of the steels [2,4,6-9]. The danger of Cr-rich particles rests not only in the formation of Cr-

depletion zones, but they can also start an electrochemical reaction between the carbide and the matrix. The corrosion resistance is subsequently reduced due to this process [10]. Although all procedures of the heat treatment are well performed, some unwanted precipitates can be present in austenitic steel after long-term aging like $M_{23}C_6$ (mainly for unstabilized steels [2,11]), Laves, and Sigma (mainly for stabilized and low-carbon steels [9, 12]). Ohmura et. al. [13] showed that $M_{23}C_6$ dominates in the steel AISI 316 (0.05C-0.014Ti-17.6Cr-11.19Ni, contents of elements are given in wt %) after long-term aging. Källqvist and Andrén [12] have detected the precipitation of NbC which prevents the formation of $M_{23}C_6$ in the AISI 347 steel (0.054C-0.78Nb-17.69Cr-11.36Ni). Kyung Seon Min and Soo Woo Nam [14] have reported that $M_{23}C_6$ is also present in the AISI 321 steel (0.03C-0.257Ti-17.90Cr-9.15Ni) stabilized with Ti additionally to the TiC particles.

Nowadays, corrosion properties of austenitic steels can be well predicted using modeling. However, the most reliable data were obtained by corrosion tests. Most of the corrosion experiments were done after aging of the steels in the temperature range of 500-950°C for up to 70 000 h [2,4,15,16]. Sometimes it is important to test components after long-term service in corrosion environments to obtain the most realistic information about microstructure stability and corrosion behavior of the steels. For this reason EPR and weight loss tests were preformed in the present work on three samples made from different austenitic steels aged for several years in power plants.

EXPERIMENTAL

In this work, the steels 18Cr-8Ni, 18Cr-10Ni, and 21Cr-30Ni (Table 1) were investigated after service for long time in a hot corrosion environment. The working conditions of tubes used for machining the experimental samples are shown in Table 2.

Table 1 Chemical compositions of investigated steels [wt. %]

Steel	C	Mn	Si	Cr	Ni	Mo	Ti	Nb	S	P
18Cr-8Ni	0.06	1.67	0.62	18.48	8.37	0.30	-	-	0.025	0.030
18Cr-10Ni	0.10	1.59	0.74	17.71	9.32	0.52	-	0.56	0.026	0.030
21Cr-30Ni	0.12	0.6	1.00	21.02	30.07	0.25	0.45	-	0.005	0.030

Table 2 Exposure conditions and average grain sizes for investigated steels

Steel	Temperature of exposure (°C)	Duration of exposure (year)	Average grain size (μm)
18Cr-8Ni	600	3.5	65 ± 27
18Cr-10Ni	650	10	20 ± 5
21Cr-30Ni	800	3	89 ± 18

Light microscopy observations were done after preparing the metallographic samples by grinding, polishing (1 μm finish) and etching in 10 % aqueous solution of oxalic acid. A light microscope NEOPHOT 30 was used to document the microstructure of the samples inclusive the determination of the average grain size by the line method. Particles precipitated in the steels were identified by transmission electron microscopy (TEM) of thin foils using the selected area electron diffraction (SAED). All samples were also studied with scanning electron microscopy (SEM) using a microscope JEOL JSM 7000F/FEG equipped with an energy dispersive X-ray (EDX) analyzer INCA OXFORD. To obtain secondary electron

imaging (SEI) micrographs and to create compositional SEM/EDX maps the operating voltage of 20 kV was used.

Two types of corrosion tests were used to determine the steel sensitization. The double loop (DL) electrochemical potentiokinetic reactivation (EPR) test was performed according to the ASTM G 108 standard. In the first step the surface was polarized anodically (from -700 to +500 mV), then the scanning direction was reversed (from +500 to -700 mV). The ratio I_R/I_A, where I_R is the maximum current in the reactivation loop and I_A is the maximum current in the anodic loop, was used as a measure of the degree of sensitization [17]. The samples can be classified into 4 sensitivity groups after the test, as it was proposed by Číhal [18]. To characterize the sensitization caused by chromium carbides the oxalic acid etch test was used (ASTM 262 practice A test). The samples were etched electrochemically in the 10% aqueous solution of oxalic acid for 90 s at ambient temperature using the current density of 1 A/cm^2. The following criteria were applied to classify the steel sensitivity to the intergranular corrosion: (a) the step microstructure, when the grain boundaries are not attacked by corrosion, (b) the dual microstructure, when the grains are not completely surrounded by deeply etched boundaries, (c) the ditch microstructure, when at least one grain is completely surrounded by deeply etched boundaries [17].

RESULTS

To get an overview of the microstructure, the samples were observed with light microscopy. For steels 18Cr-8Ni, 18Cr-10Ni and 21Cr-30Ni the micrographs and the average grain sizes (standard STN EN ISO 643 [19] was used for the grain size determination) are summarized in Figure 1 and Table 2, respectively.

The phases identified in the steels are summarized in Table 3. It was shown using TEM that the precipitates in the 18Cr-8Ni steel are $M_{23}C_6$ (Figure 2) and σ. Besides $M_{23}C_6$ and σ (Figure 3) the intragranular NbC particles were also found in the steel 18Cr-10Ni. In the 21Cr-30Ni steel, the TiC precipitates and the large intergranular $M_{23}C_6$ particles were identified (Table 3). Clusters of various particles were observed as shown in Figure 4. In comparison to the matrix, the large dark particles contain more chromium, the smaller brighter particles more titanium.

According to the EPR test (Table 4), only the 18Cr-8Ni steel with I_R/ I_A = 33.35% was classified to be severe sensitized. The limit for the severe sensitization is 30% [17, 18]. The 18Cr-10Ni steel was medium sensitized, and the 21Cr-30Ni steel retained to be passive (I_R/ I_A = 0.38 %). The oxalic acid etch test (ASTM 262-A) showed similar results (Table 4). In the sample 18Cr-8Ni, all grain boundaries were found to be completely over attacked after the test (Figure 5[a]). The corrosion level was classified as ditch. For this level, boundaries of at least one grain have to be completely over attacked (i.e. “closed”). The 18Cr-10Ni steel (Figure 5[b]) showed also a ditch microstructure, although some grains were not “closed”. The microstructure of the 21Cr-30Ni steel was classified as the dual type after the test (Figure 5[c]).

Table 3 Secondary phases identified in austenitic matrix of steels 18Cr-8Ni, 18Cr-10Ni, and 21Cr-30Ni using TEM and EDX

Steel	**Secondary phases identified**	
	Intergranular area	**Intragranular area**
18Cr-8Ni	$M_{23}C_6$ + Sigma	$M_{23}C_6$
18Cr-10Ni	$M_{23}C_6$ + Sigma	NbC
21Cr-30Ni	$M_{23}C_6$ + TiC	TiC

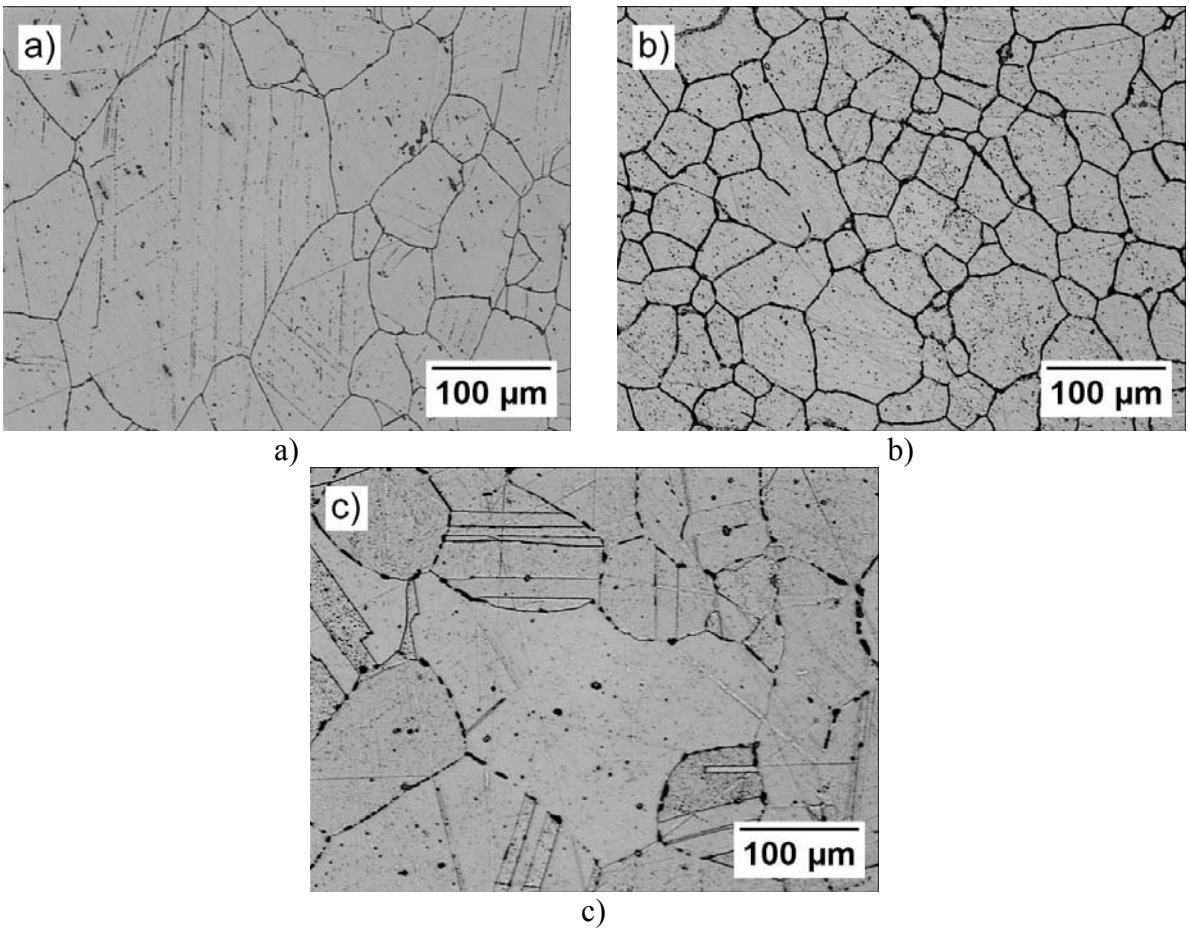

a) b)

c)

Figure 1 *Microstructures of the 18Cr-8Ni (a), 18Cr-10Ni (b) and 21Cr-30Ni (c) steels, 10% aqueous solution of oxalic acid, light microscopy.*

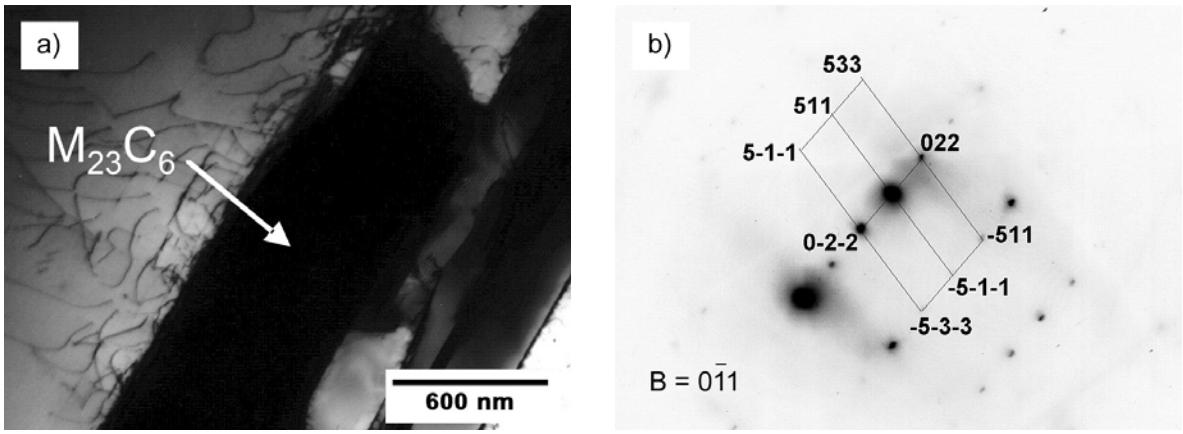

a) b)

Figure 2 *$M_{23}C_6$ particle in the 18Cr-8Ni steel (a) and corresponding electron diffraction pattern (b), TEM/SAED, thin foil.*

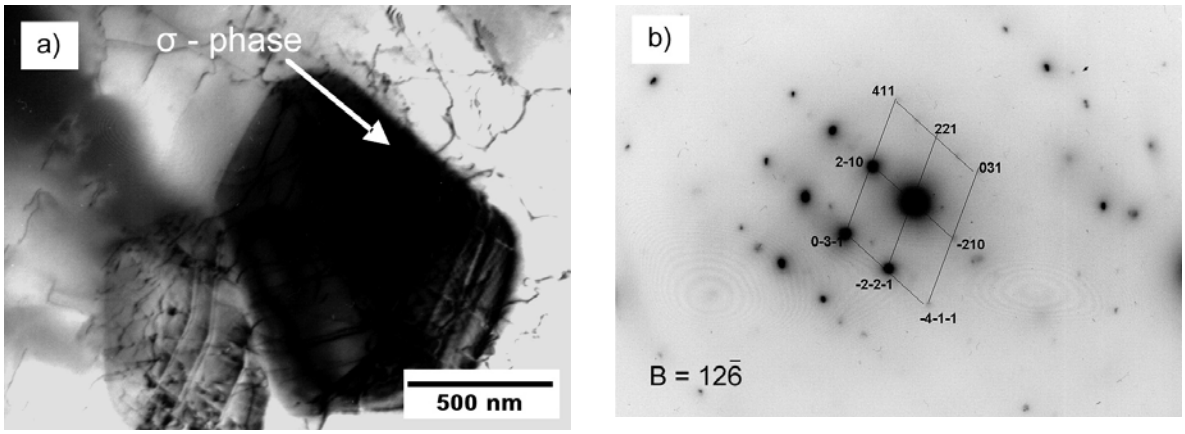

a) b)

Figure 3 *Sigma phase particle in 18Cr-10Ni steel (a) and corresponding electron diffraction pattern (b), TEM/SAED, thin foil.*

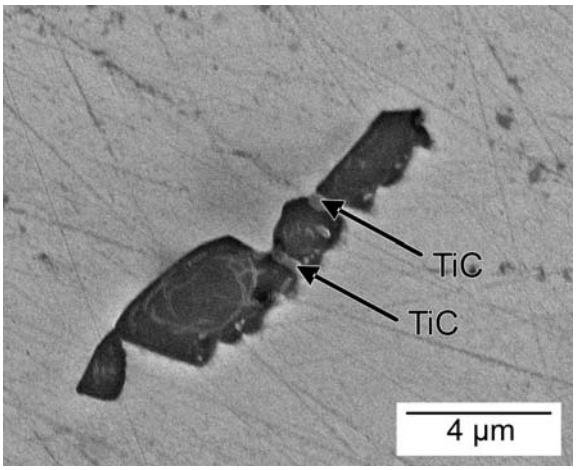

Figure 4 *Cluster of carbide particles, SEI image.*

Table 4 Results of DL-EPR and ASTM 262-A tests for investigated steels

Steel	I_R [mA/cm^2]	I_A [mA/cm^2]	I_R/ I_A [%]	DL-EPR test classification -	ASTM 262-A test classification
18Cr-8Ni	26.2	78.6	33.35	severe sensitized	ditch structure
18Cr-10Ni	11.5	98	11.73	medium sensitized	ditch structure
21Cr-30Ni	0.58	151.7	0.38	unsensitized	dual structure

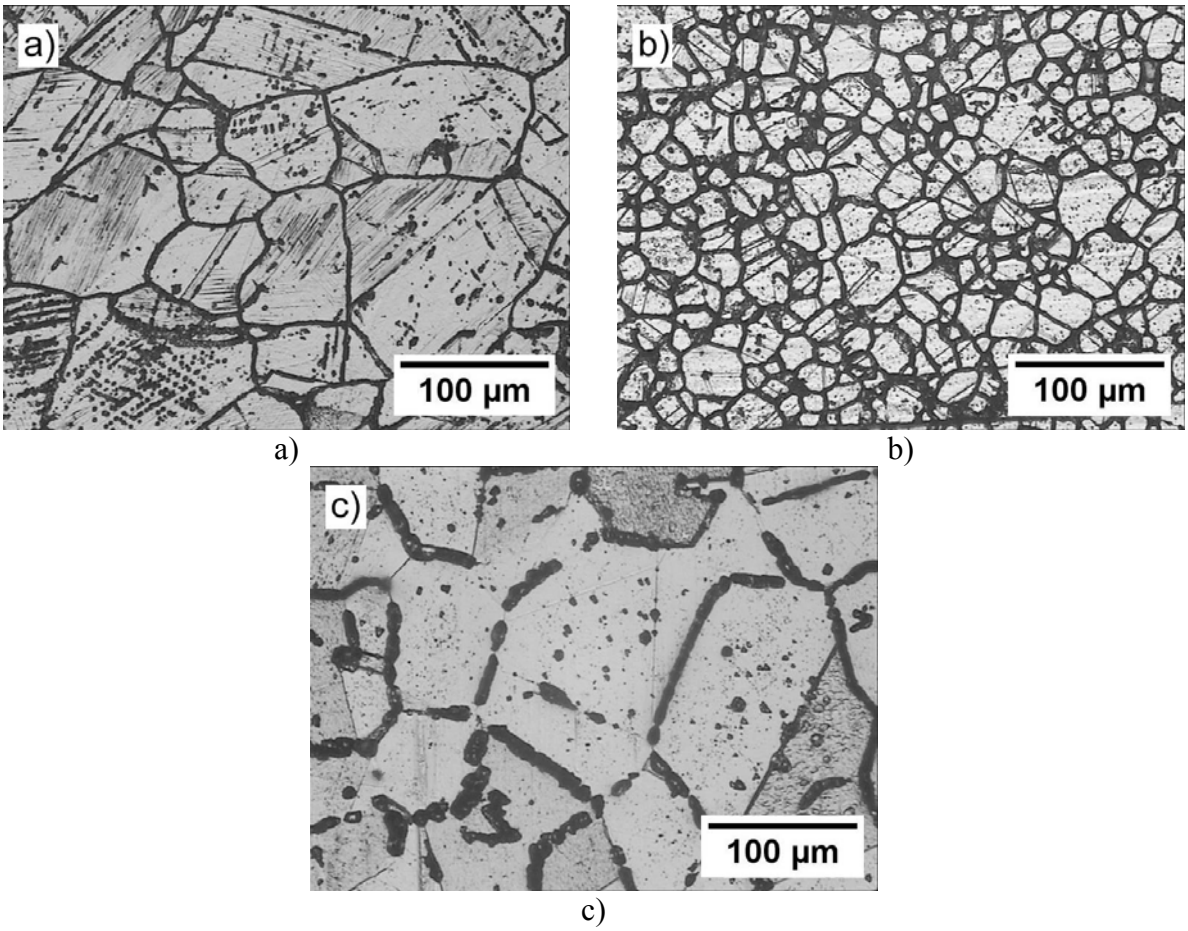

Figure 5 *Microstructures of 18Cr-8Ni (a), 18Cr-10Ni (b), and 21Cr-30Ni (c) steels after corrosion test performed according to ASTM 262 - A. In the microstructure of steel 18Cr-10Ni, the non-attacked segment of grain boundary is marked with arrow.*

DISCUSSION

Although the initial microstructures of the investigated steels are unknown, one can suggest that the non-stabilized 18Cr-8Ni steel did not contain almost any precipitates after solution heat treatment (1020-1120°C) and rapid cooling. The microstructures of stabilized steels 18Cr-10Ni and 21Cr-30Ni contained probably MC particles after stabilization treatment at temperatures between 950-1070°C and slow cooling [5]. Naturally, the precipitation of new particles and the evolution of the original particles can be expected during the long-term service (Table 2). These processes surely had an effect on the corrosion resistance of the steels investigated.

Particles of $M_{23}C_6$ form mostly dense layers along the grain boundaries in austenitic steels. In dependence on annealing temperature and/or time, the particle sizes were found to range between 50 and 1200 nm [15, 20]. Presence of large particles at the grain boundaries evokes the suggestion that the steel is sensitized. However, austenitic steels were reported to be strongly sensitized even if the particles were extremely small and therefore hardly observable by light microscopy. Small particles arranged close to each other along the grain boundaries appear in austenitic steels already after low temperature annealing [21]. The case described above was also confirmed experimentally in this work for the 18Cr-8Ni steel (Figure 1[a]). The small densely arranged intergranular particles mostly of $M_{23}C_6$ type (Figure 2, Table 3) precipitating during the service [2, 11] caused a severe sensitization of this steel. It was confirmed by both the EPR-DL and the etch tests (Table 4, Figure 5[a]). It is generally known that $M_{23}C_6$ evokes the formation of Cr-depletion zones more often than Sigma. Contrary to the Sigma particles, the $M_{23}C_6$ particles are forming continuous layers along the grain boundaries promoting the creation of large and continuous Cr-depletion zones [15]. Sigma particles precipitate in the first place on the triple-points of the austenitic microstructure [3] and do not create usually continuous Cr-depletion zones. The more extreme service conditions (compare steels 18Cr-8Ni and 18Cr-10Ni, Table 2) caused the Ostwald ripening [22] of intergranular particles (Sigma - Figure 3 and $M_{23}C_6$) precipitated in the 18Cr-10Ni steel. As a consequence, larger discrete particles more distant from each other appeared. It prevented them probably from forming a continuous depletion zone along the grain boundaries. Moreover, $M_{23}C_6$ particles were limited in growth, because of the partial stabilization of the 18Cr-10Ni steel with niobium. The NbC precipitation reduced the bulk amount of carbon needed for the substantial growth of $M_{23}C_6$. The experimental evidence about the described processes follows from the corrosion tests. Steel 18Cr-10Ni was found to be less sensitized than the 18Cr-8Ni steel according to both tests performed (Table 4, Figure 5[a] and [b]). In spite of the presence of niobium, medium sensitization instead of unsensitized state was observed for the 18Cr-10Ni steel. It was probably caused by the incorrect stabilization of this steel. The ratio between the bulk niobium and carbon contents has to be at least 8:1 according to Bhadeshia and Honeycombe [23, 24] and even 10:1 according to Sourmail [9]. This ratio for the 18Cr-10Ni steel is about 6:1 only.

At the grain boundaries of the 21Cr-30Ni steel, huge particles with dimensions often exceeding 10 μm were observed (Figure 1[c]). The more precise investigation based on the SEM/EDX mapping discovered a cluster character of these “particles”. The clusters are formed by large $M_{23}C_6$ particles containing mostly chromium and smaller particles of TiC (Figure 4). Precipitation of $M_{23}C_6$ in a Ti-stabilized steel was also reported by Kyung Seon Min and Soo Woo Nam [14]. In this work, the clusters were also observed in the grain interior of the 21Cr-30Ni steel (Figure 1[c]). The microstructure of the 21Cr-30Ni steel was classified as unsensitized according to the EPR-DL test. More factors can contribute to good resistance of this steel to the intergranular corrosion. The accelerated diffusion at high enough service temperature (800°C) enabled intensive changes in the initial microstructure consisting probably of austenitic grains containing TiC particles. As a consequence, discrete particles and/or clusters along the grain boundaries were formed due to the Ostwald ripening. It extended the grain boundary areas free of carbides and reduced in this way the areas suitable for the formation of Cr-depletion zones. Because of shorter times needed for the chromium compensation at 800°C, the continuous deeply etched boundaries were not observed all over the grain boundaries after the oxalic acid etch test (Figure 5[c], Table 4). The good etching ability of some grain boundary segments in 21Cr-30Ni steel was caused by at least two factors: the presence of “wide” clusters at the boundaries and the lattice misfit at the carbide/matrix interface.

Two methods of corrosion tests were compared in this work. It was stated that the EPR-DL method is finer scaled and more precise than the oxalic acid etch test (Table 4). The results obtained confirmed that the latter test is suitable for first-step consideration of the resistance of austenitic steels to intergranular corrosion. For a more precise screening, the EPR test should be done.

CONCLUSION

Three austenitic steels (18Cr-8Ni, 18Cr-10Ni, and 21Cr-30Ni) exploited for long-terms at temperatures between 600 and 800°C were characterized using corrosion tests and the experimental identification of phases. The results obtained can be summarized as follows:

1. Small densely arranged intergranular particles mostly of $M_{23}C_6$ were found to form continuous Cr-depletion zones in 18Cr-8Ni steel. The steel was classified as severe sensitized.
2. At the grain boundaries of 18Cr-10Ni steel larger (due to the Ostwald ripening), discrete particles were observed additionally to small densely arranged particles. The steel was classified as less sensitized compared to 18Cr-8Ni steel.
3. In 21Cr-30Ni steel, huge discrete clusters often exceeding 10 μm were observed at the grain boundaries. The clusters consisted of large Cr-rich $M_{23}C_6$ and small Ti-rich MC particles. The steel was classified as unsensitized.
4. It was confirmed that the EPR-DL method is finer scaled and more precise than the oxalic acid etch test.

Acknowledgement

The authors of the work wish to thank to the Grant Agency of the Ministry of Education and Slovak Academy of Sciences (VEGA) for financial support of the project No. 1/0126/08.

References

[1] PADILHA, A.F., PLAUT, R.L., RIOS, P.R. Annealing of Cold-worked Austenitic Stainless Steels. In *ISIJ International,* 2003, **43**, 135.

[2] TERADA, M., ESCRIBA, D.M. Investigation on the Intergranular Corrosion Resistance of the AISI 316L(N) Stainless Steel After Long Time Creep Testing at 600°C. In *Materials Characterisation*, 2008, **59**, 663.

[3] PADILHA ,A.F., ESCRIBA, D.M., MATERNA-MORIS, E., RIETH, M., KLIMENKOV, M., Precipitation in AISI 316L(N) During Creep Tests at 550 and 600 °C up to 10 Years. In *Journal of Nuclear Materials*, 2007, **362**, 132.

[4] YAE KINA, A., SOUZA, V.M., TAVARES, S.S.M., SOUZA, J.A., DE ABREU, H.F.G. Influence of Heat Treatments on the Intergranular Corrosion Resistance of the AISI 347 Cast and Weld Metal for High Temperature Services. In *Journal of Materials Processing Technology* 2008, **199,** 391

[5] *ASM Metals Handbook Volume 4 Heat treating*, Materials Park, OH: ASM International, 1991, p. 1682.

[6] PADILHA, A.F., RIOS, P.R. Decomposition of Austenite in Austenitic Stainless Steels. In *ISIJ International*, 2002, **42**, 325.

[7] MAGULA, V., LIAO, J., IKEUCHI, K., KURODA, T., KIKUCHI, Y., MATSUDA F. New Aspects of Sensitization Behavior in Recent 316 Type Austenitic Stainless Steels, In *Transactions of JWRI*, 1996, **25**, 49.

[8] KASPAROVA, O.V. The Break-down of the Passive State of Grain Boundaries and Intergranular Corrosion of Stainless Steels. In *Protection of Metals*, 1998, **34**, 520

[9] SOURMAIL, T. Precipitation in Creep Resistant Austenitic Stainless Steels. In *Materials Science and Technology*, 2001, **17**, 1.

[10] ZÁHUMENSKÝ, P., JANOVEC, J., DOMÁNKOVÁ, M., MAGULA, V. Evolution of Secondary Phases in 18Cr-12Ni-3Mo Steel During Ageing at 650-900°C In *Kovové Materiály*, 1998, **36**, 309.

[11] TANAKA, H., MURATA, M., ABE, F., IRIE, H. Microstructural Evolution and Change in Hardness in Type 304H Stainless Steel During Long-term Creep In *Materials Science and Engineering*, 2001, **A319-321**, 788.

[12] KÄLLQVIST, J., ANDRÉN, H.O. Microanalysis of a Stabilised Austenitic Stainless Steel After Long Term Ageing In *Materials Science and Engineering*, 1999, **A270**, 27.

[13] OHMURA, T., SAWADA, K., K. KIMURA, K., TSUZAKI, K. Alteration in Nanohardness of Matrix Phase Associated with Precipitation During Long-term Aging of Type 316 Stainless Steel. In *Materials Science and Engineering*, 2007, **A 489**, 85.

[14] KYUNG SEON MIN, SOO WOO NAM. Investigation of the Effect of the Types and Densities of Grain Boundary Carbides on Grain Boundary Cavitation Resistance of AISI 321 Stainless Steel Under Creep–fatigue Interaction. In *Journal of Nuclear Materials*, 2003, **322**, 91.

[15] JANOVEC, J., GRMAN, J., ORSZÁGHOVÁ, J., ŠEVC, P., ZÁHUMENSKÝ, P., PATSCHEIDER, J., TULEJA, S., PECHA, J., BOGYÓ, M., BLACH, J., MAGULA, V. Role of M23C6 Carbide Precipitation and Phosphorus Grain Boundary Segregation in Intergranular Fracture and Corrosion of 18Cr-12Ni Austenitic Stainless Steel. In *Canadian Metallurgical Quarterly*. 2002, **41**, 357.

[16] PARDO, A., MERINO, M.C., COY, A.E., VIEJO, F., CARBONERAS, M., ARRABAL, R. Influence of Ti, C and N Concentration on the Intergranular Corrosion Behaviour of AISI 316Ti and 321 Stainless Steels. In *Acta Materialia*, 2007, **55**, 2239.

[17] *ASM Metals Handbook Vol. 13: Corrosion* 9th ed. Materials Park, OH: ASM International, 1987, p. 489.

[18] ČÍHAL, V., ŠTEFEC, R. On the Development of the Electrochemical Potentiokinetic Method. In *Electrochimica Acta*, 2001, **46**, 3867.

[19] STN EN ISO 643, Steels – Micrographic determination of the apparent grain size Brussels, BE: CEN, 2003.

[20] ZÁHUMENSKÝ, P., ŠEVC, P., JANOVEC, J. Kinetika rastu medzikryštálových castíc M23C6 v austenitickej nehrdzavejúcej oceli 18Cr-12Ni-2,5Mo. In *Kovové materiály*, 1999, **37**, 108.

[21] JANOVEC, J., BOGYÓ, M., BLACH, J., ZÁHUMENSKÝ, P., VÝROSTKOVÁ, A. Splitting of AISI 316 Austenitic Stainless Steel. In *Canadian Mettalurgical Quarterly*, 2001, **40**, 97.

[22] OSTWALD, W. Über die vermeintliche Isomerie des roten und gelben Quecksilberoxyds und die Oberflächenspannung fester Körper. In *Zeitschrift für Physikalische Chemie*, 1900, **34**, 495.

[23] BHADESHIA, H.K.D.H., HONEYCOMBE, R. In *Steels Microstructure and Properties*, Burlington, VT: Elsevier, 2006, 280.

[24] SCHWEITZER, P.A., *Fundamentals of metallic corrosion*. Boca Raton, FL: CRC Press, 2007, 154.